Purging Flow Protection of Infrared Telescopes

E. P. Muntz* and M. Hanson†
University of Southern California, Los Angeles, California

The use of a purging gas flow as a means of protecting the cryogenic optics in space infrared telescopes from condensible gaseous contaminants has been studied. The significance of both the purge/contaminant differential scattering cross section and the purge gas density distribution is analyzed. It is concluded that it is important to use the correct form of the differential scattering cross section as well as accurate purge gas density distributions when estimating the effectiveness of purging flows for contaminant protection. Experimental verification of the techniques that are used here to calculate purge gas density distributions are presented. Complete contaminant rejection from the interior of a telescope is unlikely, since for realistic purge gas densities most of the contaminants prevented from reaching the optical surfaces will condense on the telescope's internal optical baffling. Specific examples of contaminant shielding for two modes of purge gas injection are presented for the Cirris I telescope. The effectiveness of helium and neon as purge gases is compared.

Introduction

THE possible contamination of space infrared telescopes mounted on the Shuttle Orbiter has been described by Simpson and Witteborn.[1] One form of contamination, the condensation of atmospheric gases (primarily O atoms at Shuttle altitudes) and Shuttle-generated gases (primarily water vapor) on cryogenic optical surfaces is the subject of this paper. Simpson and Witteborn, and more recently Guttman et al.,[2] indicate that condensation could present a serious problem to successful infrared telescope operation by affecting the scattering characteristics of the primary mirror or by causing unwanted absorption features in the infrared spectrum.[1] An additional difficulty suggested by Simpson and Witteborn may be recombination emission from the O atoms as they become O_2 after deposition. One intuitively appealing method for dealing with the contamination by condensible gases is to provide a purge flow of incondensible gas from the telescope. In practice, since the purge gas must effectively not condense, it can be either helium or neon. Purging protection has been analyzed theoretically by Murakami[3] and studied experimentally by Hetrick et al.[4]

Although it is always possible to reject contaminants by massive purging, there are several reasons why such action is not desirable. First, typical telescope systems relying on stored liquid helium for refrigeration produce on the order of 10^{-1} g/s of boiloff; consequently, there is some sort of natural upper limit defined for these systems. For systems with associated refrigerators, the purge gas has to be carried and stored. Mass flows of 10^{-1} g/s are equivalent to 36 kg per 100 h mission. There are two additional constraints present in many infrared telescopes. The most critical, which appears to be only an artifact of current design, is that the purge gas can cause relatively high pressures to be experienced in the "vacuum" dewar that thermally insulates the cryogenic portions of the telescope. In two current designs, these dewars are vented at the telescope entrance aperture. Thus, injecting purge gas into the telescope barrel can cause the vacuum envelope to experience a relatively high pressure, which in turn may cause unacceptably high heat-transfer rates. The third side effect of purge systems is that high telescope purge gas pressures may lead to serious thermal short circuiting inside the telescopes. For instance, the sensors are generally held at lower temperatures than the optical baffling and primary mirror.

Presented as Paper 82-0294 at the AIAA 20th Aerospace Sciences Meeting, Orlando, Fla., Jan. 11-14, 1982; submitted Sept. 20, 1982; revision received July 25, 1983.

*Professor, Aerospace Engineering. Fellow AIAA.
†Research Assistant. Student Member AIAA.

For these reasons, massive purging to cover the uncertainties in the purge's effectiveness is not always possible. The results discussed in the paper were obtained when two infrared telescope designers required more detailed information than was available in 1980. High-speed ambient contaminants directed antiparallel to the telescope axis are the most difficult to attenuate using a purge. The work reported here concentrated on this particular aspect of the purging protection of space infrared telescopes. A system that protects the telescope in this situation will be more than sufficient for Shuttle-generated contaminants of approximately equal or less molecular mass.

At least four space infrared telescope systems have been proposed. The important dimensions of the four are shown schematically and approximately in Fig. 1. On all of the systems the telescope barrels are held at 20-50 K with the sun shades at higher temperatures. A number of possible protection modes have been studied for these systems and are illustrated schematically in Fig. 2. The Cirris I telescope, for instance, had a ring injection system comprised of 40 orifices in a plenum encircling the exit aperture. The normals to the orifices are pointed toward the telescope axis and intersect it at an angle ω. Behind the mirror, ring and optics package mounted injections have been investigated for the SIRE telescope. The object of the ring injection schemes is to achieve a high purge number density as far as possible from the primary mirror. This is desirable since the single scatter of the relatively massive, high-speed atmospheric O atoms by a light purge gas is confined to a narrow cone about the direction of the incoming contaminant.[2] An obvious extension of the ring injection scheme is to mount it far away from the telescope aperture. This has not yet been examined in detail, but might encounter difficulties with Shuttle-generated contaminants entering the gap between the ring and the telescope.

Previous Work

Studies of the effect of cryodeposits on low-scatter mirrors have been reported by several authors.[5-7] These results, obtained for the most part using a normal incidence molecular beam, have shown that mirror degradation due to cryodeposits is a complicated story. However, for our present purpose it is perhaps important only to note that the most consistent increase in the scatter with cryodeposit thicknesses was for O_2. No data are available for incident O atoms at energies approaching those experienced in flight. Also, it has been observed that there is a significant reduction in the sticking coefficient with the increasing incident energy of the condensing species. Murakami[3] has presented an analytical study of contaminant attenuation by a purge gas system. This

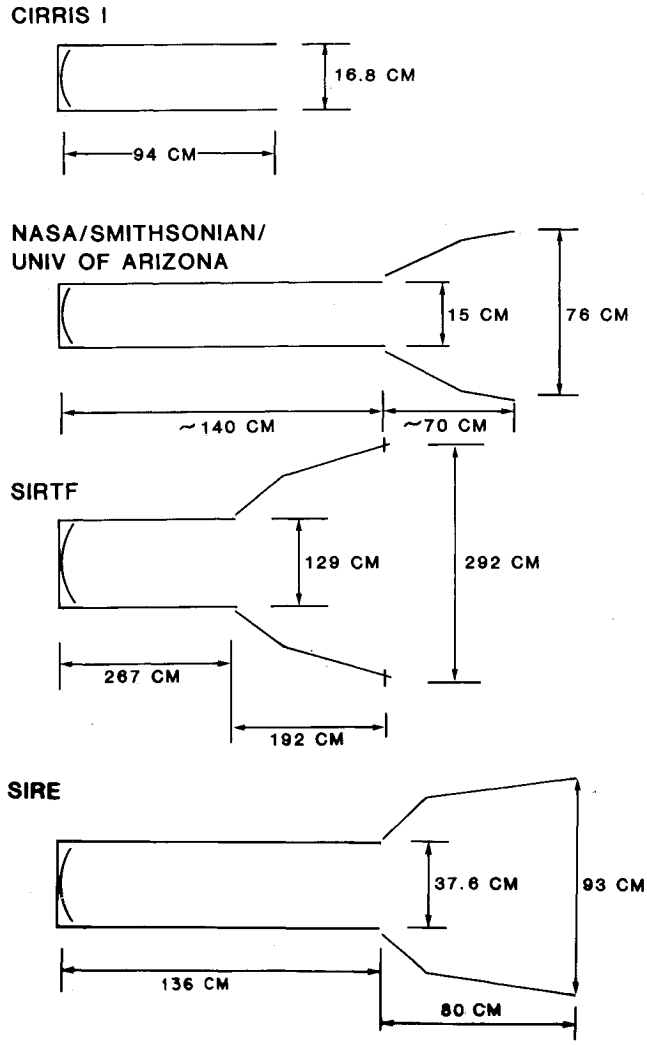

Fig. 1 Approximate internal dimensions for several infrared telescope designs.

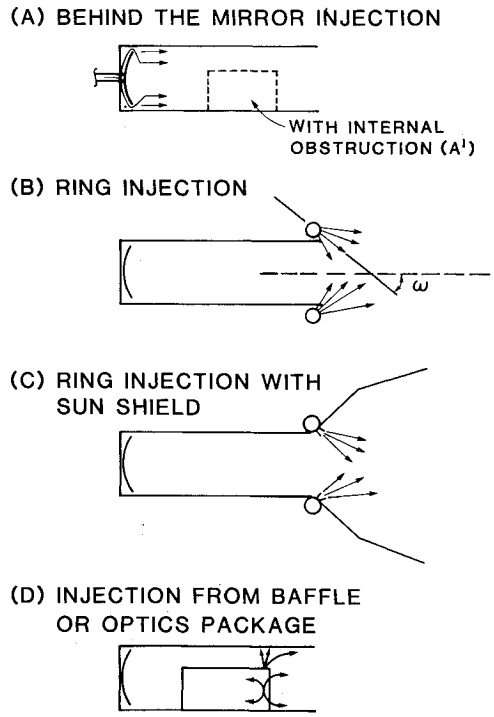

Fig. 2 Methods of injecting purge gas for contaminant protection.

analysis is in terms of hard-sphere collision cross sections. Calculations of attenuation are presented for a water vapor contaminant at 300 K and a 20 K helium purge. The purge gas Mach number is assumed parametrically to be 0.1 or 1. The analysis is intended only for low-speed entering contaminants and does not appear to be suitable for other than contaminant-background collisions that are essentially isotropic in the telescope's geometric space.

To about the same level of approximation as was used by Murakami, the deflection angle in telescope coordinates due to a collision is related to the center of mass angle by

$$\Theta = \tan^{-1} \frac{\sin\chi}{\gamma + \cos\chi - (U_p/U_c)} \tag{1}$$

where χ is the deflection angle in center of mass coordinates, γ the molecular mass ratio of contaminants to purge ($\gamma = m_c/m_p$), and U_p and U_c the purge and contaminant speeds, respectively, along the telescope axis (assuming there are no significant speeds normal to the axis). From Eq. (1) we see that, for a hard sphere (which implies a differential scattering cross section independent of χ), collisions will be isotropic in geometric space when $\gamma - U_p/U_c$ is zero. This is approximately the case when, for instance, two gases have the same molecular weight and are at the same temperature so that $\gamma \approx U_p/U_c \approx 1$. The $\gamma - U_p/U_c \approx 0$ condition is never well approximated in the telescope problem except in the unlikely situation of $m_c \ll m_p$. Particularly, it is not well approximated for ambient atmospheric molecules that have speeds of around 8 km/s, as is the case with the Shuttle Orbiter. For the incoming oxygen atoms and a 20 K helium purge, $U_p/U_c \to 0$, $\gamma = 4$, and the entire scattering is restricted to a cone with a half-angle of only 14.5 deg. As a result, the most likely event is a scattering to the inner walls of the telescope barrel where, because of the optical baffling, it is assumed that the O atoms are trapped by multiple reflections and thus condense. Short of having a continuum flow of purge gas, the high-speed contaminants are not rejected, but rather simply deflected. For Shuttle-originated contaminants such as water vapor (which has a thermal velocity distribution at about room temperature), the mass ratio still dominates, but the scattering will be somewhat more isotropic in the telescope coordinates because of the relatively finite random motion of the purge atoms. In addition, the random motion of the Shuttle contaminants will carry a significant proportion of those entering the telescope aperture to the walls, roughly in inverse proportion to the solid angle subtended by the mirror at the aperture.

A second analysis, by Guttman et al.,[2] has addressed the question of ambient oxygen atoms impinging on a helium purge for the SIRE telescope. Calculations are presented using a hard-sphere collision cross section that is introduced parametrically, with the total cross section varying between 10^{-17} and 10^{-15} cm^2. An experimental study of atmospheric contaminant shielding by purging flow has been reported by Hetrick et al.[4] In this experiment, helium was used as a purge gas in a one-tenth scale model of the SIRTF[8] telescope. Several species of ions were projected at the model from an ion gun about 1 m from the aperture of the model telescope's sun shade.

In addition to the work mentioned above, which was primarily concerned with the purging flow protection of infrared telescopes, there is an extensive literature of related studies concerning the background gas penetration of underexpanded jets. It is from this work that a more general perspective can be obtained about the characteristics of the purge gas/contaminant gas interaction. Compargue in France,[9,10] Rebrov and his co-workers in the Soviet Union,[11,12] and Muntz and his colleagues in the United

States[13-17] have studied various aspects of the invasion of a background or contaminant gas into a plume of gas expanding into a low-pressure region. For our purposes here, it is worthwhile to review those physical concepts useful in helping to understand the flow phenomena that are significant in purging applications.

There are two important dimensions associated with the penetration of background species into a gas plume. Consider the general case of a gas at a source pressure p_s expanding through an orifice into a low-pressure background gas at pressure p_B. The connection to telescope purging can be made by imagining a telescope barrel inside the source, the source pressure and temperature of which are such that they provide exit conditions identical to those of the telescope barrel. One of the important dimensions is the distance from the exit aperture along the plume centerline at which the background concentration has been reduced to e^{-1} of its value far from the source. This distance is called r_p. The other distance is the length of travel of a typical source or jet molecule in the background before it has experienced a collision with a background molecule. This distance is called r_λ. In both cases, these distances can be nondimensionalized with the source exit diameter D used as a characteristic length to give R_p and R_λ. For the case of sufficiently high pressure in the source and a sufficiently low pressure in the background, simple expressions can be developed[13] for R_p and R_λ. These simple expressions have been validated by more rigorous analysis and by experiment.[14,15]

The flow regime of the interaction between a gas plume and its background can be described by a so-called plume Knudsen number where $Kn_p = R_\lambda / R_p$. For $Kn_p < 0.1$, the plume background flow is in the continuum regime with relatively thin shock waves and mixing layers. For $Kn_p > 1$ the background gas can more or less freely penetrate the plume up to a distance R_p from the source. For conditions where $R_p < 1$, the background gas begins to penetrate into the source itself. Other things being equal, the distance R_p is controlled by the pressure p_s (or number density $n_s = p_s / kT_s$),

$$R_p = CV_{\text{rel}} n_s \Omega_{Bj} D / \bar{C}_B \equiv CV_{\text{rel}} (D/\lambda_{Bj}) / \bar{C}_B$$
$$\equiv CV_{\text{rel}} Kn_{Bj}^{-1} / \bar{C}_B \qquad (2)$$

where C is a constant,[17] V_{rel} a typical relative collision speed between the background and jet molecules, $\bar{C}_B$ the mean background speed directed at the source, and Ω_{Bj} the background and jet molecule collision cross section. Also, λ_{Bj} is the mean free path of a contaminant or background molecule in the source gas and $Kn_{Bj} = \lambda_{Bj}/D$ is a type of source Knudsen number.

Flow conditions where $R_p \approx 1$ have been extensively investigated by Deglow and Muntz[16,17] and by Brook et al.[18] However, it is when $R_p < 1$ that is of interest in the case of the purging protection of infrared telescope optics. This flow regime has not yet been studied in great detail, although some information has recently become available.[19] Results in Ref. 19 show that, even for $Kn_{Bj} = 0.1$ and a thermal background with about the same molecular mass as the source gas, there is a significant background penetration into the source region. Thus complete rejection of contaminants from a telescope would require very high telescope barrel purge densities. Molecular flow with $R_p \ll 1$ is not of interest because it does not offer sufficient protection and thus permits essentially free penetration of the source.

Analysis

In order to predict purge gas effectiveness, the purge gas density and velocity fields must be known. Also, reliable collision cross sections appropriate to the particular species and collision energies are necessary. Reliable differential scattering cross sections as a function of energy are now available for the He-O system.[20]

In the present work, purge gas density fields and pressures were measured for laboratory-scale models using several possible injection configurations. Argon was used as the laboratory purge gas. The configurations studied are shown in Fig. 2. The measurements have been compared to simplified predictions in order to help establish convenient methods for predicting full-scale purge gas density fields. Where the prediction techniques were found to be unreliable, the laboratory results were scaled directly to the full scale.

Scaling the Purge Flow from Laboratory to Full Scale

From the flowfield experiments, measurements of purge gas mass flow, number density distributions, and pressures in model telescopes are available. The experiments were done using a reduced-scale model with argon as the purge gas and a wall temperature of about 290 K. In order to calculate the amount of protection provided for full-scale telescopes, the laboratory purge flow results must be scaled to a full-size telescope with helium (or possibly neon) and a more typical wall temperature of 20 K. For system design what is required are the relationships between the full-scale number density distributions and the purge gas mass flows.

Consider the flow of a rarefied gas in the telescope. For internal flows, following Kogan[21] or the discussion in Ref. 22, the characteristic quantities of the flow are L, a geometric length scale; $\bar{C}$, the mean thermal speed of the molecules based on the telescope wall temperature T_w; and n_0, the characteristic molecular number density in the flow. For a given scale change, the characteristic densities are related by the requirement for equal Knudsen numbers. The Knudsen number can be expressed as $Kn = \lambda / L$, where λ is the purge gas self-collision molecular mean free path in a coordinate system attached to the telescope. Note that this is a Knudsen number different from the plume Knudsen number of the previous section. In this case, Kn relates to the self-collisions between the purge gas atoms. The plume Knudsen number Kn_p relates only to the interaction between the purge gas and the contaminants. It can be shown that, for purposes of determining the purge gas flow properties, the contaminant flow can be ignored since it typically exchanges only a small amount of momentum with the purge gas. Noting that $\lambda = (\Omega n_0)^{-1}$ (Ω is the collision cross section),

$$\frac{(n_0)_{\text{FS}}}{(n_0)_{\text{EXP}}} = \frac{\Omega_{\text{EXP}}}{\Omega_{\text{FS}}} \frac{L_{\text{EXP}}}{L_{\text{FS}}} \qquad (3)$$

the corresponding mass flow for the full-scale telescope is

$$\dot{M}_{\text{FS}} = m_{\text{FS}} \dot{N}_{\text{EXP}} \frac{L_{\text{FS}}}{L_{\text{EXP}}} \frac{\Omega_{\text{EXP}}}{\Omega_{\text{FS}}} \frac{\bar{C}_{\text{FS}}}{\bar{C}_{\text{EXP}}} \qquad (4)$$

In the above expressions the collision cross sections are for purge gas self-collisions and are evaluated at the characteristic temperatures $T_{w\text{EXP}}$ or $T_{w\text{FS}}$ using viscosity data.

Purge Gas Density or Pressure Predictions

For various practical reasons, the purge gas densities must generally be low; thus, free molecular flow conditions are at least approximated in the anticipated practical applications (a purge self-collision mean free path greater than the telescope diameter). Accordingly, it is appropriate to compare the experimental results to the predictions based on the assumption of free molecular flow. The flow in the telescope barrel is also assumed to be independent of the presence of a sun shade since the typical sun shade has a large area compared to the telescope's barrel. At the exit aperture of the telescope barrel, it is assumed that the mass flow from the telescope can be derived from the random motion of the purge gas, with no

return mass flow due to the sun shade reflections. With this assumption, the exit aperture number density is given by

$$n_E = \frac{1}{2}\left(\frac{2}{mkT_w}\right)^{1/2}\frac{\dot{M}}{a^2} \tag{5}$$

where a is the radius of the exit aperture, $\dot{M}$ the mass flow, m the molecular mass, k the Boltzmann constant, and T_w the telescope barrel temperature. The factor of ½ appears in Eq. (5) because it has been assumed that at the exit aperture there are no purge atoms returning to the telescope barrel. Once n_E is known, it is easy to calculate the density field outside the barrel aperture for installations without a sun shade. At any point (x,y,z),

$$n(x,y,z) = \int_{A_E} \frac{n_E \cos\Theta}{4\pi R^2}\, dA_E \tag{6}$$

where Θ is the angle between the outward normal to the exit area element dA_E and the vector defined by dA_E and the point (x,y,z). The distance R is from dA_E to (x,y,z). Positive z is outward along the telescope's optical axis.

In the tube it is assumed that there are no radial gradients, only longitudinal ones. The density distribution is defined in standard references[23] by the axial number density gradient for finite tubes. It is useful to express the centerline number densities in a nondimensional form, using the primary mirror radius (assumed to be equal to the barrel aperture radius) as a characteristic length and $2n_E = n(L)$ as the characteristic number density. Inside the barrel

$$n'(z') = 1 + \tfrac{3}{8}[1 + (8/3L')](L' - z') \tag{7a}$$

and outside the barrel (assuming no influence of the sun shade), Eq. (6) becomes

$$n'(z') = \frac{1}{2}\left(1 - \frac{1}{[1 + (z' - L')^{-2}]^{1/2}}\right) \tag{7b}$$

where the primes represent nondimensional length and nondimensional number densities. Note that the exact free molecular number density field can be solved using the techniques described by Patterson.[24] For our present purposes this does not appear to be necessary since the major difference between the exact prediction and the one used here will extend only about 1 diam upstream of the exit aperture.

For the case of ring injection with no sun shade (e.g., Cirris I), the flowfield outside of the telescope can be found by using the source flow analogy of Ashkenas and Sherman.[25] The flow in the injection orifices has a relatively low Knudsen number, so this should be a reasonable approximation. Assuming no collisions between the intersecting jets, the contributions from each of the injection orifices are summed at any point to give the local number density.

The densities induced in the telescope barrel by the ring injection scheme are more difficult to determine by simple analytical means. In the present case the experimental results have been used to provide the appropriate densities.

Attenuation Calculation

Using calculated and empirically derived purge gas density distributions whose accuracy will be examined in the following sections, attenuation calculations have been made for several injection configurations. The calculations rely on the following assumptions:

1) The 20 K purge gas is stationary compared to the 8 km/s speed of the contaminant gas.

2) The helium-oxygen atom differential scattering cross sections are reliably given by Harvey and Herm's calculations.[20]

3) Only single scattering is important for events that scatter contaminants outside of the mirror.

Using these assumptions, an analysis of the attenuation gives for the coordinate system shown in Fig. 3,

$$\frac{(n_c U_c)_m}{(n_c U_c)_\infty} = R_m^{-2}\int_0^{R_m}\int_0^{2\pi}\exp\left\{-\int_\infty^0\int_{R_m}^\infty\int_0^{2\pi}[I(\Theta) \times n(r,\phi,z)\cos\Theta/R^2]\, r_m\, dr_m\, d\phi_m\, dz\right\} r\, dr\, d\phi \tag{8}$$

The present analysis differs from Ref. 2 in that it is based on a direct determination of the number of atoms that are scattered and miss the mirror, rather than those that scatter and hit. This avoids the difficulties associated with the rapidly increasing small-angle differential scattering cross sections and permits convenient reintroduction of those contaminants not scattered beyond the mirror into the unscattered beam. Since the contaminants not scattered outside the mirror are assumed to remain in the original beam direction, the calculations are conservative from the point of view of taking small amounts of multiple scattering into account. The calculated attenuations would be somewhat greater if multiple scattering were permitted.

A further assumption is that the contaminants missing the mirror are trapped on the inner walls of the telescope. Certainly, it is not likely that the O atoms will be trapped in one wall encounter. However, the optical baffling makes it reasonable to assume that a contaminant atom will experience a large number of wall encounters, thus increasing the likelihood of condensation before reaching the mirror in a random walk down the telescope walls. The behind-the-mirror injection scheme would be effective in removing these migrating contaminants, whereas the ring injection scheme would not, since with ring injection there would be no purge gas mass motion in the telescope barrel. We have not tried to estimate these effects, but have assumed the contaminants stick at the axial position where they hit the telescope walls. The question of recombination radiation from the wall condensate should also be considered, but is beyond the scope of the present work.

Model Design and Experimental Facilities

SIRE Model

A quarter-scale model of the SIRE telescope was used in this study (see Fig. 1 for approximate full-scale dimensions). It is accurate in detail as far as the internal configuration of the telescope is concerned. The internal envelope of the telescope is modeled by a series of aluminum rings that are interspaced by 0.36 mm (0.014 in.) thick washer-like

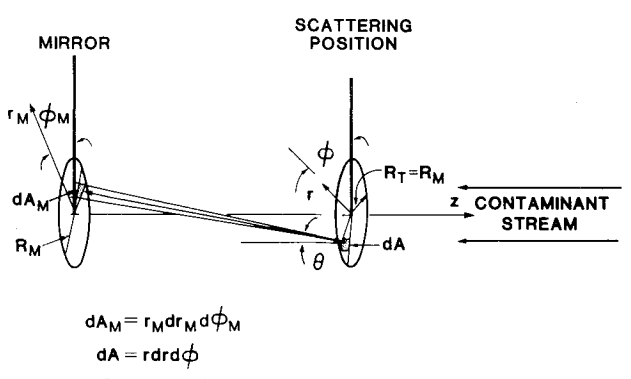

Fig. 3 Coordinates used for describing contaminant attenuation.

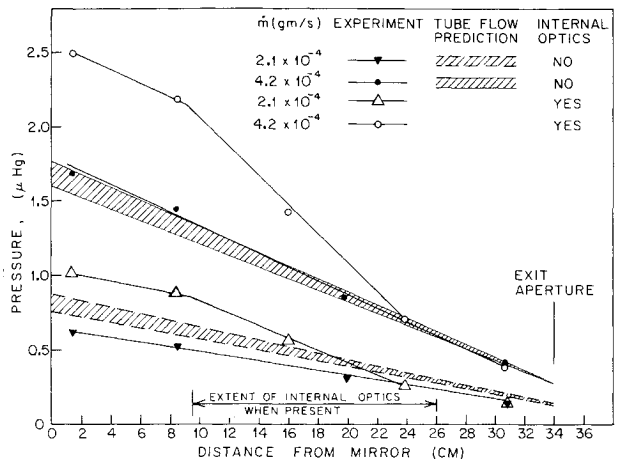

Fig. 4 Comparison of model wall pressure measurements to predictions for no internal optics; also shown are measurements with the SIRE optics package in place (predictions are for free molecule flow with the gradients corresponding to both the average internal diameter and the minimum or mirror end diameter).

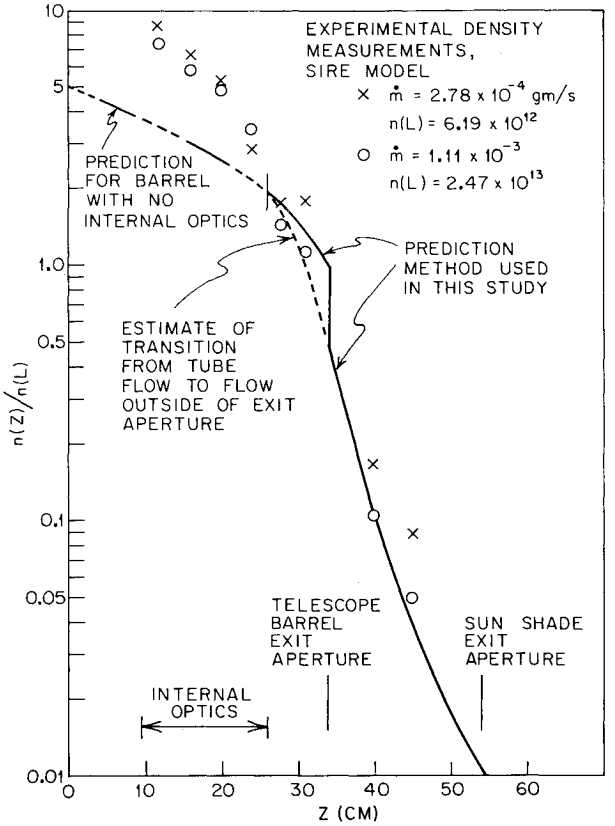

Fig. 5 Axial density measurements compared to prediction (prediction does not include internal optics; mesurements were made with internal optics installed).

aluminum sheets used to model the optical baffles. The centerbody that contains the secondary optical components is mounted in the model such that it can be externally rotated through 180 deg using a geartrain. The aluminum rings and washers are nested in an external tube and clamped with a retaining nut at the sun shade end. At the mirror end of the model, a completely modeled mirror and inlet flow passage has been provided.

In the walls of the telescope and sun shade there are 12 penetrations of 1.5 mm diam by which an electron beam is brought into the interior of the telescope. The gas density is measured by observing the intensity of the fluoresence excited by the electron beam.[26] Points along the length of the beam are observed through windows in the model wall. Pressure measurements can also be made at several points along the walls of the telescope tube using an MKS Baratron.

The model is suspended in a high-vacuum facility about 2 m in diameter and 3 m long. The facility has LN_2-cooled walls and is pumped by a 20 K gaseous helium cryopump. With the model installed, the pressure in the vacuum tank reaches 10^{-7} Torr after about 1 h of cryopumping. There is also an auxilliary LN_2-trapped diffusion pump [61 cm (24 in.) in diameter] attached to the facility.

When there is flow through the model, the facility pressure is about 5×10^{-6} Torr for the largest mass flow used in the experiments. For this condition, the pressure at the exit aperture of the telescope is about 5×10^{-4} Torr. Thus, there is a factor of 10^{-2} between the tank and telescope aperture pressures.

Cirris I Model

The SIRE model was modified at the exit aperture of the model telescope's barrel to become a 1/1.78 scale Cirris I telescope. The sun shade was removed and a model of the Cirris I aperture configuration substituted for the retaining nut of the SIRE model.

External purge gas injection was to be used for Cirris I. The Cirris I injection configuration is a series of 40 holes placed in an injection manifold around the exit aperture at a full-scale radius of 14.2 cm from the optical axis. The orifices were oriented such that in various experiments the normal to the exit plane formed angles of 30 and 60 deg with the telescope axis. This angle is called ω, with positive ω indicating the flow is directed in toward the optical axis of the telescope as indicated in Fig. 2. In the Cirris I experiments the density field created by the injection was measured using the electron beam densitometer. Also, pressure measurements were made at several stations inside the telescope, the most important being at the position of the dewar vent, which is 3.6 cm from the injection orifices toward the mirror for the full-scale telescope.

Results

Comparison of Predicted Purge Gas Densities and Pressures to Experiments

It is of interest to obtain an estimate of the accuracy of the previously described methods for predicting the density or pressure fields by applying them to the model telescope flows. Using Eqs. (5) and (7a) the model exit pressure and telescope barrel density or pressure gradient can be predicted for a given mass flow. Comparisons of the experimental wall pressures with the predictions based on the mass flows measured using a positive displacement technique are shown in Fig. 4 for the SIRE model with and without internal optics. For the lower mass flow case, the average Knudsen number based on the barrel diameter is ≈ 1.5. The measurements and predictions agree quite well. Because the telescope barrel internal diameter decreases somewhat toward the mirror, the predictions are based on the exit diameter for $p(L)$ and on both the average and mirror end diameters for the pressure gradient. The agreement between experiment and prediction is consistent with the experimental uncertainties. It is expected that the pressure will fall below the prediction of Eq. (7a) over a distance of about one upstream diameter from the exit aperture. The high mass flow results are not quite as good an approximation of free molecule flow, but do not exhibit a significant disagreement with the prediction, which is as expected.[27] Notice that the internal optics package has a blockage effect on the flow, but that downstream of the package its presence is not detectable.

Density measurements inside the SIRE model with the optics package installed are compared to the predictions of Eq. (7) in Fig. 5. There is excellent agreement where it is

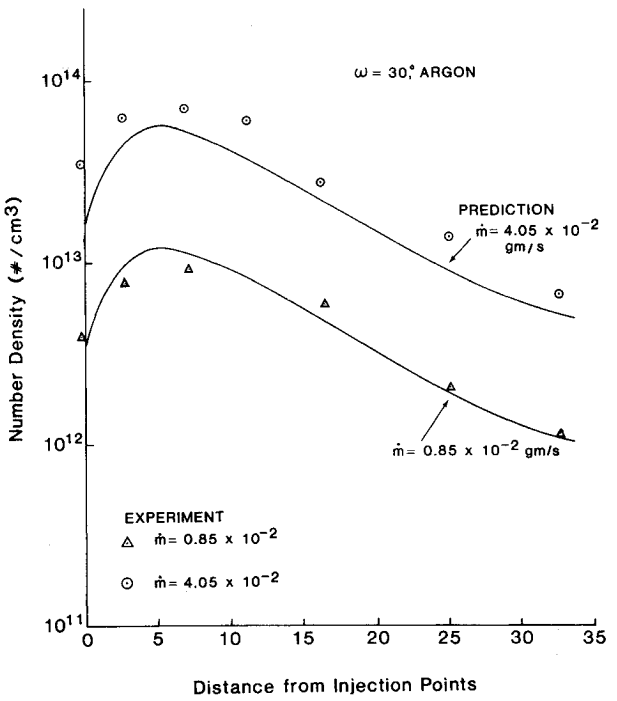

Fig. 6 Comparison of model axial density measurements to prediction for ring injection.

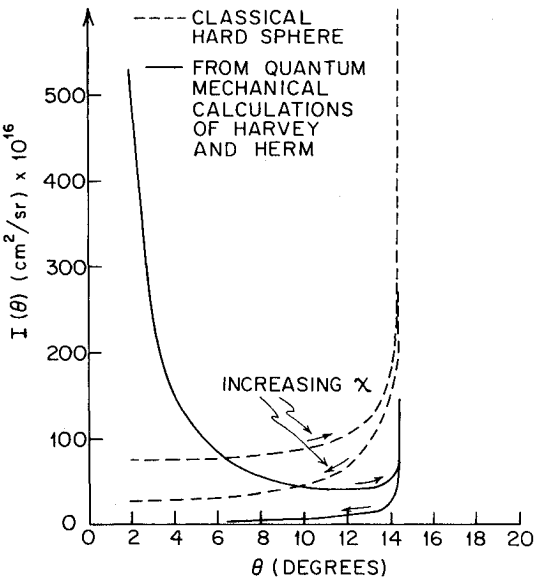

Fig. 7 Differential scattering cross sections for He-O as a function of the telescope geometric angle Θ.

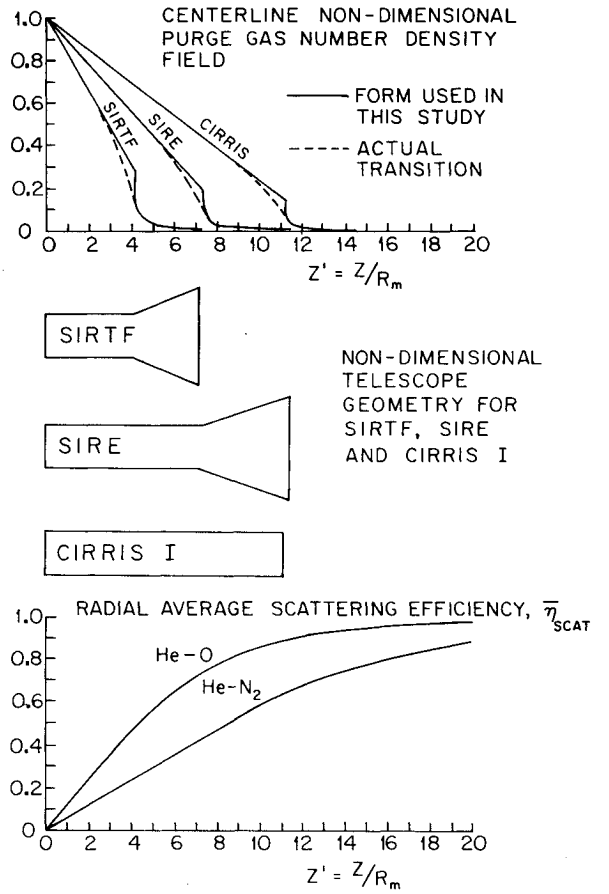

Fig. 8 Radially averaged efficiency for scattering outside of the mirror as a fraction of all scattering events at a given position; comparison is made to density distribution of purge gas for behind-the-mirror injection for three telescopes (non-dimensional coordinates as described in the text with the three telescopes shown to scale).

expected, downstream of the optics package and in the sun shade area.

From the pressure measurements it is concluded that the free molecule predictions outlined previously are a good description of purge gas flowfields when the purge gas average Knudsen number is of order one. Ignoring the presence of the typical SIRE sun shield does not lead to any significant predicted density errors, at least on the centerline (Fig. 5). This would not be the case if the sun shield had a noticeably smaller area relative to the telescope barrel.

For the Cirris I ring injection mode we made predictions as described before. Comparisons between the experimental density measurements and the predictions are shown in Fig. 6 for $\omega = 30$ deg and two mass flows. Here there is excellent agreement at the low mass flow and reasonable agreement at the higher mass flow. The departure of the data above the prediction in the higher mass flow case has been shown by other experiments to be due to the collision effects in the purge gas. The points in Fig. 6 that are slightly to the mirror side (negative distance) of the purge gas injection orifices are derived from wall pressure measurements at a location corresponding to the position of the aperture leading to the Cirris I dewar volume. The order of magnitude of these pressures can be verified by calculating the collision frequency within the colliding purge gas jets.

Importance of Purge Gas Density Distribution and Collision Cross-Section

The center of mass differential scattering cross section for the He-O system as transformed[23] to the telescope coordinates (assuming a relative speed of 8 km/s and stationary helium atoms) is shown in Fig. 7. Also included in Fig. 7 is the corresponding hard-sphere differential cross section. The total cross section at any geometric angle Θ is the sum of the contributions from the two branches that result from grazing and head-on type collisions. Note that there is a considerable shape difference between the hard sphere and the actual cross sections, with the hard sphere being relatively constant compared to the actual curve.

The limited scattering angles possible because of the mass ratio [Eq. (1)] are important when considering the purge gas density distribution. In order to illustrate the point, we have calculated radially averaged scattering efficiencies ($\bar{\eta}_{SCAT}$) for the SIRE, Cirris I, and SIRTF telescopes. Here, the scattering efficiency is defined as the ratio of the contaminants scattered

outside the mirror to the total number of scattering events at any particular location. Thus, $\bar{\eta}_{SCAT}$ depends only on geometry and is an indicator of the efficiency with which the purge gas number density at a given location scatters a particular type of contaminant. These results were obtained for an assumed constant differential cross section in telescope coordinates, up to the limiting scattering angle. This assumption is convenient and is reasonable because the exact shape is not important for the present illustrative purposes. For the three telescopes, both the purge gas density distributions (assuming behind-the-mirror injection and no internal optics in all cases) and $\bar{\eta}_{SCAT}$ are presented in Fig. 8 using the nondimensional coordinates described earlier [Eqs. (7)]. The $\bar{\eta}_{SCAT}$ results are for both He-O and He-N_2 to illustrate the effect of the contaminant mass.

The total scatter cross section at any axial position times $\bar{\eta}_{SCAT}$ gives the effective scattering cross section at that position. This is seen to vary significantly over the distributions of the purge gas densities from the three telescopes. It is very important to use the correct purge gas axial density distribution since, for example, a scatterer at $z' = 10$ is about eight times as effective as one at $z' = 1$ for He-O. We also emphasize that none of the telescopes have a significant purge density downstream of their barrel's exit aperture.

Calculated Purge Effectiveness

Calculations of the purge gas shielding of Cirris I have been made for the two injection configurations, behind the mirror and the ring, using both reduced and complete forms of Eq. (8). The accuracy of the calculations are, of course, limited by the assumptions detailed in a previous section, as well as the accuracy of the density fields that are derived from Eqs. (6) and (7). Also, for the ring injection, densities in the telescope barrel were derived from experimental pressure measurements scaled to full-size. The ring injection densities outside the barrel were calculated as discussed before.

The calculations are summarized in Table 1. To assist in the summary we have presented the results in terms of the attenuation achieved by the purge gas in the form,

$$(n_c U_c)_m / (n_c U_c)_\infty = \exp - G\dot{M} \tag{9}$$

where G is a geometric/collision cross-section factor and has units of s/g. Examination of Eq. (8) shows that Eq. (9) is valid only if the density distribution scales linearly with the mass flow and retains the same shape. It is also valid only if no radial and azimuthal average is taken or if the radial and azimuthal variations in contaminant transmission are small. Although the G factor has no mathematical significance for a radially averaged attenuation, Table 2 shows that the performance of a given configuration does not change very much when radially averaged values are computed. Therefore, comparison of various systems on the basis of centerline G factors is reasonable. For convenience, our discussion will consider only the transmission of the contaminants incident along the telescope axis. With this restriction the form of Eq. (9) is correct. For the ring injection method, the purge gas densities vary linearly with the mass flow up to the limiting mass flows that depend on the angle ω. Beyond this, the linear assumption is in error but in a direction that causes underestimations of the purge gas effectiveness.

Note that G is a measure of the purge effectiveness per unit mass flow. Table 1 shows that the behind-the-mirror injection is considerably more efficient in the use of purge gas, being about 15 times more efficient than the $\omega = 60$ deg ring injection. On the other hand, Table 3 gives the purge gas transmission when a limit of 5×10^{-5} Torr is set for the Cirris I dewar pressure. In this case, it can been seen that the ring injection method is able to achieve significantly greater attenuation of the ambient atmosphere, albeit with the need for much larger mass flow. The dewar pressure was assumed to be the pressure of the 20 K gas at the telescope exit. In effect, this assumes that the dewar is at 20 K. Less attenuation would be realized if the dewar temperature were assumed to be some average between its inner and outer wall temperatures.

We have also studied the effect of assuming a hard-sphere collision, which implies a constant differential scattering cross section in the center of the mass coordinates. The actual and hard-sphere cross sections are shown in Fig. 7. The results for behind-the-mirror injection of helium into the Cirris I telescope give for O atoms a hard-sphere G of 3.39×10^4 compared to the actual G of 1.14×10^4. In both cases the total cross section is the same. There is an increase of a factor of about three in G resulting from the assumption of isotropic scattering in the center of mass coordinates. Clearly, it is important to use the correct shape of the scattering cross section in this type of calculation.

Finally, the effect of purge gas type was investigated, with He and Ne compared on the basis of hard-sphere interactions. The neon G for behind-the-mirror protection of Cirris I from O atoms is 5.3×10^4 compared to 3.39×10^4 for helium. There appears to be only a modest difference in G for these two gases. However, on a volume flow basis the Ne would be much more effective than the He. This implies that Ne will provide satisfactory contaminant shielding using behind-the-mirror injection for the 5×10^{-5} Torr dewar pressure limit, with a mass flow of around 6.3×10^{-4} g/s and an O atom transmission of approximately 1.2×10^{-5}. In this calculation, the neon G was obtained by multiplying the actual He G from Table 1 by the ratio of neon and helium hard-sphere G ($1.14 \times 10^4 \times 5.33/3.39$).

The effect on the attenuation of locating the ring injection point at increasing distances from the Cirris I exit aperture was investigated. Moving the ring one telescope length (94 cm) from the exit aperture increased the G due to the plume by

Table 1 Effect of injection mode

Injection method	G
Behind mirror	1.14×10^4
Ring, $\omega = 60$ deg	7.38×10^2
Ring, $\omega = 30$ deg	5.60×10^2
Ring, $\omega = 0$ deg	2.83×10^2

Table 2 Effect of radially averaging the attenuation as opposed to centerline calculation only

Injection method Ring	Total transmission Centerline	Radial average
$\omega = 30$ deg	2.26×10^{-4} ($G = 560$)	6.65×10^{-5} ($G_{eff} = 641$)

Table 3 Effect of holding the dewar pressure constant (5×10^{-5} Torr) for ring and behind-the-mirror injection

ω, deg	$\dot{M}$, (g/s)	Barrel trans.	Plume trans.	Total trans.
60	0.40×10^{-2}	0.275	1.2×10^{-1}	3.3×10^{-2}
30	1.35×10^{-2}	0.275	1.5×10^{-3}	4.1×10^{-4}
0	2.85×10^{-2}	0.275	7.6×10^{-4}	2.1×10^{-4}
Behind mirror	2.8×10^{-4}	0.45	9.0×10^{-1}	4.1×10^{-2}

about 20%, which is probably not worth the mechanical complication it would cause. This result can be anticipated by examining Fig. 8, where $\bar{\eta}_{SCAT}$ is already about 0.8 at the Cirris I exit aperture; thus, using ring injection at greater distances will result in only modest improvements. On the other hand, due to generally low values of $\bar{\eta}_{SCAT}$, the SIRTF configuration would be quite sensitive to the ring injection position even beyond the sun shade. In the case of Cirris I, moving the ring would be of benefit primarily in reducing the pressure in the dewar, thus permiting an increase in mass flow.

Comparison to Previous Work

The results obtained here can be compared only approximately to previous results. We note that the total He-O cross section found by Harvey and Herm[20] for 8 km/s is 3.7×10^{-15} cm^2. Guttman et al.[2] made hard-sphere calculations. Based on the difference in G between the hard-sphere and actual cross sections discussed above, a 3.7×10^{-15} cm^2 total actual cross section is equivalent to a hard-sphere cross section of about 1.2×10^{-15} cm^2. Thus, the results given by Guttman et al. for $\sigma_{TOT}=10^{-15}$ cm^2 in their Fig. 4 (for $l=206$ cm, $R=16.1$ cm, and $L'=12.8$) can be compared at least approximately to the present Cirris I calculations ($L'=11.2$). For an O atom transmission of 10^{-1}, the results in Ref. 2 imply a pressure at a mirror of 8.2×10^{-5} Torr. From the Cirris I G of 1.4×10^4, a mirror pressure of 10.8×10^{-5} Torr can be calculated. There is reasonable agreement between the present results and those of Guttman et al.

The results of the present work and those of Hetrick et al.[4] can also be compared, but only very approximately. From Fig. 8 we find that the average $\bar{\eta}_{SCAT}$ over the telescope barrel for Cirris I is around 0.65, while for SIRTF it is about 0.25. For behind-the-mirror injection, estimates based on the Cirris I calculation and the 2.6 times smaller $\bar{\eta}_{SCAT}$ give an effective G of around 0.44×10^4 for SIRTF. This results in a required mirror pressure of about 2×10^{-4} Torr for a transmission of 0.1, compared to the 1×10^{-5} Torr found in Ref. 4. The factor of 20 ratio between these results is so large that we feel that it is significant, despite the approximate nature of the comparison.

The mirror pressure found by Murakami[3] for 10% transmission of thermal background water vapor entering the SIRTF telescope is about 1×10^{-5} Torr for purge flows at low Mach numbers. This result compared to the present results is consistent with the notion that the high-speed ambient O atoms are considerably more difficult to attenuate than a thermal background of about the same molecular mass.

Summary

Measurements of the flow properties of purge gases in model infrared telescopes have established procedures for making reasonable estimates of purge gas densities in full scale. It has been demonstrated that it is important to use correct forms of both the purge gas density distribution and the differential scattering cross section in order to obtain reliable estimates of the purge effectiveness.

By calculation it has been shown that, at least for Cirris I, significant ambient O atom attenuation can be achieved with both the behind-the-mirror and ring injection configurations. Since the ambient O atoms are considerably more difficult to attenuate than lower-energy scattered contaminants with roughly the same mass, successful protection from all types of the lighter contaminants (H_2O, etc.) appears possible with realistic mass flows. In no case is a mass flow required that is greater than the Cirris I helium boiloff.

The behind-the-mirror injection mode is by far the most mass flow efficient. However, in terms of some specified pressure limit in the telescope, dictated say by heat-transfer considerations, the ring injection mode is superior.

Neon appears to offer a large attenuation without exceeding the dewar pressure limitations for the behind-the-mirror mode. This configuration would also be attractive because of its ability to keep contaminants requiring many wall encounters to condense from reaching the mirror.

Acknowledgment

The authors would like to thank Prof. R. Edwards for many useful discussions. The work was supported in part by a contract from Utah State University and in part by contract from Hughes Aircraft Co. Professor R. E. Kaplan and Mr. Robert Amen designed the data recording system and computer experiment control. Mr. Don Kingsbury and Mr. Casey DeVries provided the entire experimental setup.

References

[1] Simpson, J. P. and Witteborn, F. C., "Effect of the Shuttle Contaminant Environment on a Sensitive Infrared Telescope," *Applied Optics*, Vol. 16, 1977, pp. 2051-2073.

[2] Guttman, A., Furber, R. D., and Muntz, E. P., "The Protection of SIRE'S Cryogenic IR Optics in Shuttle Orbiter," *Proceedings of the Society of Photo-Optical Instrumentation Engineers*, No. 216, 1980, pp. 174-185.

[3] Murakami, M., "Theoretical Contamination of Cryogenic Satellite Telescopes," NASA Tech. Paper 1177, 1978.

[4] Hetrick, M. A., Rantanen, R. O., Ress, E. B., and Froechteningt, J. F., "Experimental Investigation of Contamination and Contamination Prevention Techniques to Cryogenic Surfaces on Board Orbiting Spacecraft," NASA CR-152171, 1978.

[5] Heald, J. H. and Brown, R. F., "Measurements of Condensation and Evaporation of Carbon Dioxide, Nitrogen, and Argon at Cryogenic Temperatures Using a Molecular Beam," AEDC TR 68-110 (AD 674596), 1968.

[6] Arnold, F., "Degradation of Low-Scatter Metal Mirrors by Cryodeposit Contamination," AEDC TR 75-128 (AD 13007022), 1975.

[7] Brown, R. F., Trayer, D. M., and Busby, M. R., "Condensation of 300-2500 K Gases on Surfaces at Cryogenic Temperatures," *Journal of Vacuum Science and Technology*, Vol. 7, 1970, pp. 241-246.

[8] Witteborn, F. C. and Young, L. S., "Spacelab Infrared Telescope Facility (SIRTF)," *Journal of Spacecraft and Rockets*, Vol. 13, Nov. 1976, pp. 667-674.

[9] Campargue, R., "Aspiration of a Single Component Gas by Penetration of a Free Jet's Shock Structure," *Comptes Rendus de l'Academie des Sciences*, Vol. 268A, 1969, pp. 1427-1430.

[10] Campargue, R., "Aerodynamic Separation Effects on Gas and Isotope Mixtures Induced by Invasion of the Free Jet Shock Wave Structure," *Journal of Chemical Physics*, Vol. 52, 1970, pp. 1795-1802.

[11] Rebrov, A., Chekmarev, S., and Sharafutdinov, R., "Influence of Rarefaction on the Structure of a Free Jet of Nitrogen," *Zhurnal Prikladnoi Mekhaniki i Tekhnicheskoi Fiziki*, Vol. 1, 1971, pp. 136-141.

[12] Rebrov, A. K., "Experimental Study of Relaxing Low-density Flows," *Progress in Astronautics and Aeronautics: Rarefied Gas Dynamics*, Vol. 51, edited by J. L. Potter, AIAA, New York, 1977, pp. 811-848.

[13] Muntz, E. P., Hamel, B., and Maguire, B., "Some Characteristics of Exhaust Plume Rarefaction," *AIAA Journal*, Vol. 8, No. 8, Aug. 1970, pp. 1651-1658.

[14] Brook, J. and Hamel, B., "Spherical Source Flow with Finite Back Pressure," *Physics of Fluids*, Vol. 15, 1972, pp. 1898-1912.

[15] Brook, J., Hamel, B., and Muntz, E. P., "Theoretical and Experimental Study of Background Gas Penetration into Underexpanded Free Jets," *Physics of Fluids*, Vol. 18, 1975, pp. 517-528.

[16] Deglow, T., "Background Gas Mixture Penetration of Underexpanded Jets, Application to Isotope Separation," Ph.D. Thesis, University of Southern California, Los Angeles, June 1977.

[17] Deglow, T. and Muntz, E. P., "Isotope Separation by Jet-Background Interaction," *Journal of Applied Physics*, Vol. 50, No. 2, 1979, pp. 589-594.

[18] Brook, J., Calia, V., Muntz, E. P., Hamel, B., Deglow, T., and Scott, P., "Jet Membrane Process for Aerodynamic Separation of Mixtures and Isotopes," *Journal of Energy*, Vol. 4, Sept.-Oct. 1980, pp. 199-207.

[19] Muntz, E. P., Qian, S-S., Duenas, R., Bejamin, D., and Shoostarian, A., "A Study of Reverse Leaks," *Rarefied Gas*

Dynamics, 13th Symposium, Plenum Press, New York, to be published.

[20]Harvey, M. M. and Herm, R., "Helium Purge Flow Prevention of Atmospheric Contamination of the Cryogenically Cooled Optics of Orbiting Infrared Telescopes; Calculation of He-O Differential Cross Section," Air Force Space Div., Rept. TR-SD-TR-81-53, June 1981.

[21]Kogan, M. N., *Rarefied Gas Dynamics*, Plenum Press, New York, 1969.

[22]Muntz, E. P. and Hanson M., "Studies of the Purging Flow Protection of Infrared Telescopes," AIAA Paper 82-0294, 1982.

[23]Kennard, E. H., *Kinetic Theory of Gases*, McGraw Hill Book Co., New York, 1939.

[24]Patterson, G. N., *Introduction to the Kinetic Theory of Gas Flows*, University of Toronto Press, Toronto, 1971.

[25]Ashkenas, H. ahd Sherman, F., "The Structure and Utilization of Supersonic Free Jets in Low Density Wind Tunnels," *Rarefied Gas Dynamics*, Vol. 215, edited by J. H. deLeeuw, Academic Press, New York, 1965, pp. 84-105.

[26]Muntz, E. P., "The Electron Beam Fluorescence Technique," AGARDograph 132, 1969.

[27]Edward, R. H., "Low-Density Flows Through Tubes and Nozzles," *Progress in Astronautics and Aeronautics: Rarefied Gas Dynamics*, Vol. 51, edited by J. L. Potter, AIAA, New York, 1977, pp. 199-224.